

Fluorescences 页面总设计 (20250607 版本) :

注:

本页面的设计包括 3 个段落, 每个段落单独设计, 图片为设计布局的参考图。

一. 段落 1

段落 1 包含: 三个区域, 各个区域的分布参考图 1, 各个区域的文字内容如下:

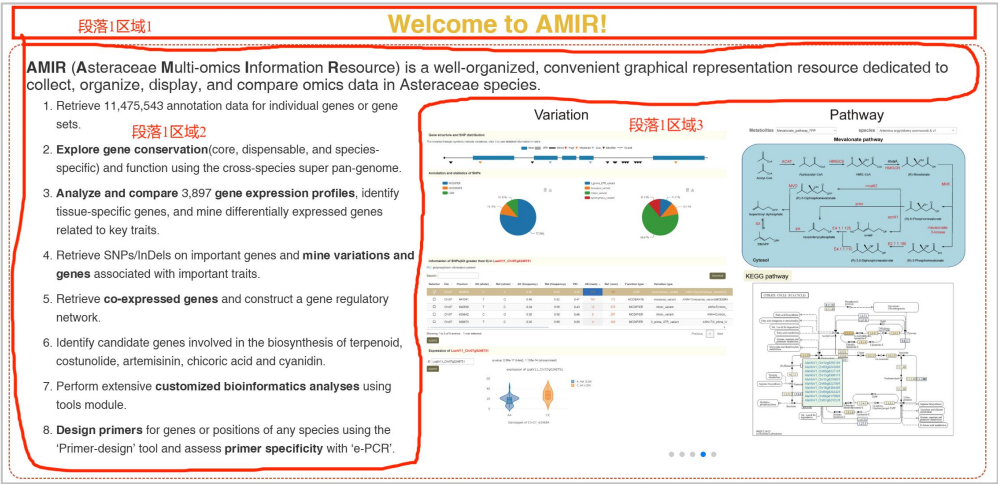


图 1

段落 1 区域 1 (标题) :

Fluorescences and Light-up RNA aptamers

段落 1 区域 2 (文本) :

Light-up RNA aptamers are fluorescent RNA molecules that become fluorescent upon binding to specific fluorophores. This concept emerged from the need for non-invasive, real-time imaging tools to study RNA molecules and their interactions within living cells. Traditional fluorescent tags like GFP (green fluorescent protein) are not suitable for RNA because they are protein-based¹. Thus, the development of RNA-based fluorescent tags (light-up RNA aptamers) became crucial for expanding the toolkit available for RNA visualization and functional studies.

1. Core Structure and Fluorescence Activation Mechanism: G-Quadruplex Platforms, Triplex Cap and Binding Pocket, Triplex Cap and Binding Pocket.
2. Three Key Mechanisms for Fluorescence Regulation: Twisted

- Intramolecular Charge Transfer (TICT), Contact Quenching (CQ), Spirolactonization (SP).
3. Cutting-Edge Technological Advances: Avidity-Enhanced Dimeric Aptamers, Logic-Gated Aptamers, Design driven by Artificial Intelligence.
4. Applications: High-sensitivity detection, Live cell RNA imaging, Multi-target synchronous imaging.
5. Challenges: Intracellular delivery, Background signal, Rational design tools.
-

段落 1 区域 3 (滑动图片) :

这部分放像“Home”页一样自动切换的图片 (Figure 1-Figure 5, 见压缩包) , 格式参考图 2, 图片下方的黑色和白色字体分别是 标题 和 副标题, 点击图片可以链接或导航到其他页面或区域。

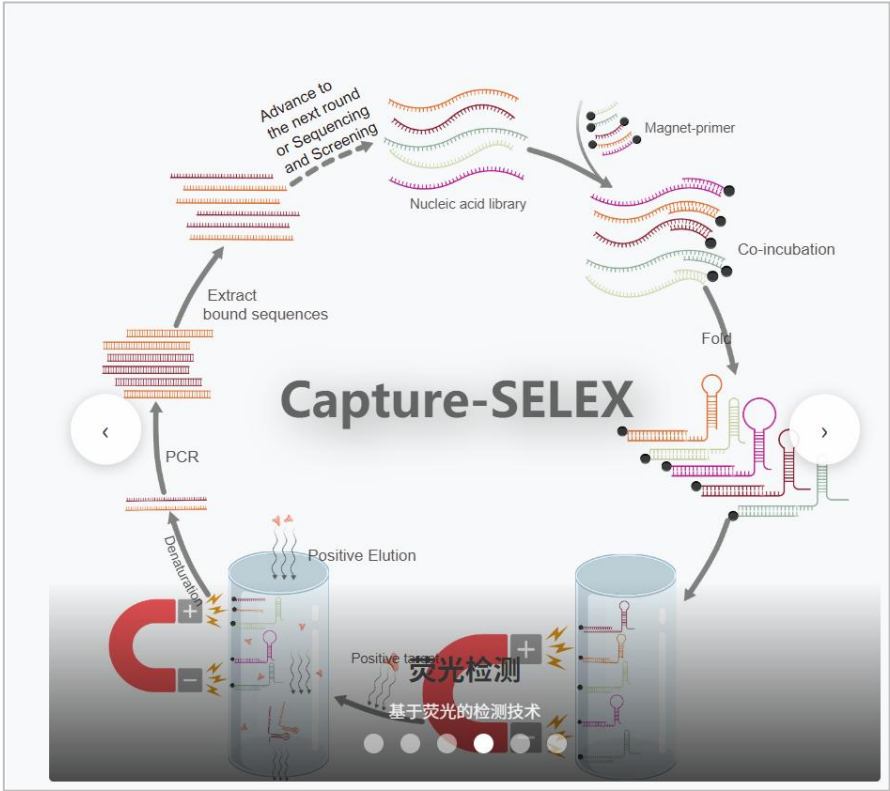


图 2

	标题	副标题	链接或导航
Figure	Core Structure	Dynamic Conformational Switching	导航到本页面的段落 3_二级标题 1

1.svg			
Figure 2.svg	Fluorescence Activation Mechanism	Twisted Intramolecular Charge Transfer, Contact Quenching and Spirolactonization	导航到本页面的 段落 3_3 级标题 1
Figure 3.svg	Light-Up RNA Aptamers	Biomedical application tools	https://aptamer.ribocentre.org/_posts/Corn-aptamer
Figure 4.svg	Structures	Secondary and tertiary structures	https://aptamer.ribocentre.org/_posts/Corn-aptamer
Figure 5.svg	Fluorescent molecules	Fluorescence based on affinity	导航到本页面的 段落 3_2 级标题 3

二. 段落 2

该段落的布局参考 Home 页的对应部分，包括一个 **搜索栏 1**，**数据统计仪表盘 1**，**数据详情表 1**，各个区域的布局如图 3 和图 4 所示，文字内容如下：



图 3



图 4

搜索栏 1:

格式如图 3 所示，其中搜索框中的文字“Enter the aptamer name, sequence or ligand...”，下方的几个关键词为：“Sequences”“Ligands”“Structures”“Mechanisms”“Applications”，点击关键词可以链接或导航到其他页面或区域，对应关系如下表。

关键词	链接或导航
Sequences	导航到本页面的段落 2_数据详情表 1
Ligands	导航到本页面的段落 3_表格 1
Structures	https://aptamer.ribocentre.org/Ribocentre-aptamer/
Mechanisms	导航到本页面的段落 3_3 级标题 1
Applications	https://aptamer.ribocentre.org/applications/

数据统计仪表盘 1:

格式参考图 3，左图柱状图 题目为“Publication Trends by Year”，右图饼图题目为“Distribution of Fluorophore Activation Mechanisms”。饼图的分类型字段参考 数据详情表 1。

数据详情表 1:

格式参考图 4，左上角标题为“Light-Up RNA Aptamers”，表中各行各列的内容参考 [Fluorescences 页面 aptamer 序列与荧光小分子等信息对应表 20250604.xlsx](#)（见压缩包）的 A-H 列（即从 Number 列到 Relevant 3D structures 列）。后面的“PubMed linker”列用作“Years”列的导航链接，“More information”列用作“Sequence name”列的导航链接（没有对应的先行先不添加导航链接）。“Mechanisms”列为饼图的分类型字段。

三. 段落 3

段落 3 从上到下依次包含：一级标题，文本 a ，二级标题 1，文本 b，图 0，图注 0(图注要紧贴上方的图片，可以与别的类型的文本格式有别，显示出与图片的一体)，三级标题 1，文本 1，图 1，图注 1，三级标题 2，文本 2，图 2，图注 2，三级标题 3，文本 3，图 3，图注 3 ，文本 4，表格 1，二级标题 2，文本 c，表格 1，参考文献。

一级标题:

Light-up RNA aptamers

文本 a:

The discovery of Spinach, the first light-up RNA aptamer, by Jaffrey and colleagues in 2011 marked a significant milestone. Spinach binds to a fluorophore called DFHBI and emits green fluorescence, mimicking GFP². Following Spinach, several other light-up aptamers were developed, including Mango, Broccoli, and Corn, each binding to different fluorophores and exhibiting different fluorescence properties^{3, 4, 5}. Researchers optimize light-up RNA aptamers for improved brightness, stability, and minimal background fluorescence. This involves iterative cycles of selection and mutation to enhance the aptamer's performance for better performance in cellular environments^{6, 7, 8}.

Light-up RNA aptamers represent a significant advancement in the study of RNA biology, offering a versatile and powerful tool for real-time imaging and functional analysis of RNA molecules in living cells⁹.

二级标题 1:

Fluorogenic mechanisms

文本 b:

Light-up RNA aptamers contain specific binding sites that interact with small-molecule fluorophores. These fluorophores are non-fluorescent or weakly fluorescent in the absence of the aptamer. Upon binding to the aptamer, the fluorophore undergoes a conformational change that enhances its fluorescence properties. This binding typically occurs through a combination of hydrogen bonding, Van der Waals interactions, and stacking interactions within the RNA's three-dimensional structure.

Understanding their mechanism of action involves exploring how these aptamers interact with their fluorophores to produce fluorescence, the structural basis of their function, and the principles guiding their design and optimization¹⁰.

图 0:

见压缩包文件

[light-up aptamer.svg](#)

图注 0:

Structural Basis: Molecular Framework for Fluorescence Activation. Aptamers precisely identify the chemical groups of fluorophores through base complementarity or structural complementarity. After binding, the excited state energy of the fluorophore is

effectively converted into fluorescence emission through the restriction of the rigid structure of the fitting body, rather than heat energy or vibration energy loss.

三级标题 1:

Twisted Intramolecular Charge Transfer (TICT)

文本 1:

TICT refers to a mechanism where the binding of a target induces a conformational change in the RNA aptamer, leading to the activation or enhancement of fluorescence through a twisted charge-transfer state. This state involves the separation of charge within the molecule, resulting in a geometry that promotes fluorescence.

In the unbound state, the RNA aptamer and its fluorophore may be in a non-planar or less twisted conformation with limited charge separation, leading to weak or no fluorescence. Upon binding to a specific target, the aptamer undergoes a conformational change that facilitates a twist between the donor and acceptor moieties within the fluorophore. This twist maximizes the charge separation, creating an intramolecular charge transfer state with a large dipole moment. The TICT state stabilizes the fluorophore in a way that enhances its fluorescence emission, often resulting in a red-shifted and intensified fluorescence signal compared to the non-twisted state.

图 1:

[*Twisted intramolecular charge transfer \(TICT\)_20260526.svg*](#)

图注 1:

TICT mechanism regulates fluorescence activation through conformational dynamics of fluorophores.

三级标题 2:

Contact Quenching (CQ)

文本 2:

Contact quenching in light-up RNA aptamers involves the reduction or elimination of fluorescence due to the close physical proximity of a quencher molecule to the fluorophore. This process is highly dependent on the spatial arrangement and interaction between the RNA aptamer and its target.

In the absence of the target, the fluorophore may be in close proximity to a quencher moiety within the RNA aptamer, resulting in minimal fluorescence. Binding of the target induces a conformational change in the RNA aptamer that separates the fluorophore from the quencher. The increased distance between the fluorophore and quencher reduces the efficiency of non-radiative energy transfer, allowing the fluorophore to emit fluorescence. The efficiency of contact quenching and subsequent fluorescence recovery can be modulated by the nature of the target-aptamer interaction and the specific design of the aptamer.

Light-up RNA aptamers exploiting contact quenching are used in biosensors to detect various biomolecules by monitoring changes in fluorescence. These aptamers facilitate the detection and quantification of analytes in complex mixtures.

图 2:

[Contact quenching \(CQ\) 20260526.svg](#)

图注 2:

CQ operates via direct physical interaction between the fluorophore and quencher.

三级标题 3:

Spirolactonization (SP)

文本 3:

Spirolactonization in light-up RNA aptamers involves the formation of a spirolactone ring structure upon binding to a target. This structural change enhances the fluorescence of the aptamer, providing a clear signal upon target recognition.

In the absence of the target, the RNA aptamer remains in a conformation that does not support spirolactone formation, leading to weak or no fluorescence. Binding of the target induces a conformational rearrangement in the aptamer, promoting the formation of a spirolactone ring. The formation of the spirolactone ring stabilizes the fluorophore in a fluorescent state, significantly enhancing its emission properties. The structural rigidity and planarity introduced by the spirolactone ring reduce non-radiative decay pathways, leading to a bright fluorescence signal.

Spirolactonization-based light-up RNA aptamers are used to detect specific targets with high sensitivity and specificity. These aptamers can serve dual functions in theranostics, providing both diagnostic imaging and therapeutic action.

图 3:

[Spirolactonization \(SP\) 20250526.svg](#)

图注 3:

SP is exemplified by rhodamine-based probes. Aptamer binding alters the local microenvironment, triggering lactone ring-opening to yield the fluorescent zwitterionic form.

二级标题 2:

Properties of Fluorophore-Aptamer pairs

文本 c:

Each light-up RNA aptamer is usually specific to a particular fluorophore. The specificity arises from the precise shape and chemical environment of the binding pocket within the RNA. The sequence and structure of the aptamer dictate the compatibility with

the fluorophore, ensuring selective binding and fluorescence activation. Researchers focused on optimizing these aptamers for improved brightness, stability, and minimal background fluorescence. This included engineering the aptamers and fluorophores for better performance in cellular environments.

The table below lists several fluorescent small molecular-RNA pairings for which interaction patterns have been known through crystallographic studies or NMR. (The table only shows the representative individuals of each type of fluorescent small molecule. For more details, click on small molecule to jump to the corresponding view.)

表格 1:

Fluorescent molecule	UPAC	Molecular Formula	Molar mass	CAS	Excitation (nm)	Emission (nm)	Aptamer	Fluorogenic mechanisms
DFHBI	(5Z)-5-[(3,5-difluoro-4-hydroxyphenyl)methylidene]-2,3-dimethylimidazol-4-one	C ₁₂ H ₁₀ F ₂ N ₂ O ₂	252.22 g/mol	1241390-29-3	469	501	Spirochrome	TICT
MG	[4-[[4-(dimethylamino)phenyl]-phenylmethylidene]cyclohexa-2,5-dien-1-ylidene]-dimethylazanium;chloride	C ₂₃ H ₂₅ CIN ₂	364.9 g/mol	569-64-2	630	655	MG aptamer	TICT
HBC530	4-[(E)-1-cyano-2-[4-[2-hydroxyethyl(methyl)amino]phenyl]ethenyl]benzonitrile	C ₁₉ H ₁₇ N ₃ O	303.4 g/mol	156840-13-0	485	530	Pepper	TICT
TO1	4-methylbenzenesulfonate; (2Z)-3-methyl-2-[(1-methylquinolin-1-ium-4-yl)methylidene]-1,3-benzothiazole	C ₂₆ H ₂₄ N ₂ O ₃ S ₂	476.6 g/mol	107091-89-4	510	535	Mango	TICT
DFHO	(5Z)-5-[(3,5-difluoro-4-hydroxyphenyl)methylidene]-3-methyl-2-(nitrosomethylidene)imidazolidin-4-one	C ₁₂ H ₉ F ₂ N ₃ O ₃	281.21 g/mol	1420815-34-4	505	545	Coron	TICT
DMHBI	5-[(4-hydroxy-3,5-dimethoxyphenyl)methylidene]-2,3-dimethylimidazol-4-one	C ₁₄ H ₁₆ N ₂ O ₄	276.29 g/mol	1629243-34-0	400	537	Chili	TICT
YO3	(2Z)-3-methyl-2-[(E)-3-(1-methylquinolin-1-ium-4-yl)prop-2-enylidene]-1,3-benzothiazole	C ₂₁ H ₁₉ N ₂ O ⁺	315.4 g/mol	-	595	620	Mango-III	TICT
ThT	4-(3,6-dimethyl-1,3-benzothiazol-3-ium-2-yl)-N,N-dimethylaniline	C ₁₇ H ₁₉ CIN ₂ S	318.9 g/mol	2390-54-7	455	485	Betroot	TICT

TMR	2-[3-(dimethylamino)-6-dimethylazaniumylidenexanthene-9-yl]benzoate	$C_{24}H_{22}N_2O_3$	386.4 g/mol	1207 18-52-7	564	587	TM R3 aptamer	CQ
DFA ME	methyl 3-[4-[(3,5-difluoro-4-hydroxyphenyl)methylidene]-1-methyl-5-oxoimidazol-2-yl]prop-2-enoate	$C_{15}H_{12}F_2N_2O_4$	322.26 g/mol	1420 815-55-9	514	619	Beetroot	TICT
OTB	3-methyl-2-[(3-methyl-1,3-benzothiazol-3-ium-2-yl)methylidene]-1,3-benzoxazole	$C_{17}H_{15}N_2OS^+$	295.4 g/mol	-	380	421	DIRs2-Apt	TICT
NBSI	(5Z)-2-[(E)-2-(4-fluorophenyl)ethenyl]-5-[[4-[2-hydroxyethyl(methylamino)phenyl]methylidene]-3-methylimidazol-4-one	$C_{22}H_{22}FN_3O_2$	379.4 g/mol	-	524	580	Clivias	TICT
TMR-DN	Tetramethylrhodamine-Dinitroaniline	$C_{37}H_{38}N_6O_{10}$	726.7 g/mol	-	545	570	RhobAST	CQ

参考文献:

- [1] Pédelacq, J. D., Cabantous, S., Tran, T., Terwilliger, T. C., & Waldo, G. S. (2006). Engineering and characterization of a superfolder green fluorescent protein. *Nature biotechnology*, 24(1), 79-88.
<https://pubmed.ncbi.nlm.nih.gov/16369541/>
- [2] Paige, J. S., Wu, K. Y., & Jaffrey, S. R. (2011). RNA mimics of green fluorescent protein. *Science (New York, N.Y.)*, 333(6042), 642-646.
<https://pubmed.ncbi.nlm.nih.gov/21798953/>
- [3] Dolgosheina, E. V., Jeng, S. C., Panchapakesan, S. S., Cojocaru, R., Chen, P. S., Wilson, P. D., Hawkins, N., Wiggins, P. A., & Unrau, P. J. (2014). RNA mango aptamer-fluorophore: a bright, high-affinity complex for RNA labeling and tracking. *ACS chemical biology*, 9(10), 2412-2420.
<https://pubmed.ncbi.nlm.nih.gov/25101481/>
- [4] Song, W., Filonov, G. S., Kim, H., Hirsch, M., Li, X., Moon, J. D., & Jaffrey, S. R. (2017). Imaging RNA polymerase III transcription using a photostable RNA-fluorophore complex. *Nature chemical biology*, 13(11), 1187-1194.
<https://pubmed.ncbi.nlm.nih.gov/28945233/>
- [5] Filonov, G. S., Moon, J. D., Svensen, N., & Jaffrey, S. R. (2014). Broccoli: rapid selection of an RNA mimic of green fluorescent protein by fluorescence-based selection and directed evolution. *Journal of the American*

Chemical Society, 136(46), 16299-16308.

<https://pubmed.ncbi.nlm.nih.gov/25337688/>

[6] Song, W., Strack, R. L., Svensen, N., & Jaffrey, S. R. (2014). Plug-and-play fluorophores extend the spectral properties of Spinach. *Journal of the American Chemical Society*, 136(4), 1198-1201.

<https://pubmed.ncbi.nlm.nih.gov/24393009/>

[7] Autour, A., C Y Jeng, S., D Cawte, A., Abdolazadeh, A., Galli, A., Panchapakesan, S. S. S., Rueda, D., Ryckelynck, M., & Unrau, P. J. (2018). Fluorogenic RNA Mango aptamers for imaging small non-coding RNAs in mammalian cells. *Nature communications*, 9(1), 656.

<https://pubmed.ncbi.nlm.nih.gov/29440634/>

[8] Zhang, Q., Su, C., Tian, X., & Zhang, C. Y. (2023). Corn-Based Fluorescent Light-Up Biosensors with Improved Signal-to-Background Ratio for Label-Free Detection of Long Noncoding RNAs. *Analytical chemistry*, 95(20), 8097-8104.

<https://pubmed.ncbi.nlm.nih.gov/37171156/>

[9] Neubacher, S., & Hennig, S. (2019). RNA Structure and Cellular Applications of Fluorescent Light-Up Aptamers. *Angewandte Chemie (International ed. in English)*, 58(5), 1266-1279.

<https://pubmed.ncbi.nlm.nih.gov/30102012/>

[10] Lu, X., Kong, K. Y. S., & Unrau, P. J. (2023). Harmonizing the growing fluorogenic RNA aptamer toolbox for RNA detection and imaging. *Chemical Society reviews*, 52(12), 4071-4098.

<https://pubmed.ncbi.nlm.nih.gov/37278064/>
